Bioorganic & Medicinal Chemistry Letters 20 (2010) 5184–5190

Contents lists available at ScienceDirect

Bioorganic & Medicinal Chemistry Letters

journal homepage: www.elsevier.com/locate/bmcl

Succinic acid amides as P2–P3 replacements for inhibitors of interleukin-1β converting enzyme (ICE or caspase 1)

Paul Galatsis [a,*], Bradley Caprathe [a], John Gilmore [a], Anthony Thomas [a], Kristin Linn [a], Susan Sheehan [a], William Harter [a], Catherine Kostlan [a], Elizabeth Lunney [a], Charles Stankovic [a], John Rubin [a], Kenneth Brady [b], Hamish Allen [b], Robert Talanian [b]

[a] Pfizer Global R&D, 2800 Plymouth Road, Ann Arbor, MI 48105, USA
[b] BASF Bioresearch Corporation, 100 Research Drive, Worcester, MA 01605, USA

ARTICLE INFO

Article history:
Received 26 March 2010
Revised 1 July 2010
Accepted 2 July 2010
Available online 8 July 2010

Keywords:
ICE inhibitor
P2–P3 replacement
Succinic acid amides

ABSTRACT

Succinic acid amides have been found to be effective P2–P3 scaffold replacements for peptidic ICE inhibitors. Heteroarylalkyl fragments occupying the P4 position provided access to compounds with nM affinities. Utilization of an acylal prodrug moiety was required to overcome biopharmaceutical issues which led to the identification of **17f**, a potential clinical candidate.

Interleukin IL-1β (IL-1β) is a pro-inflammatory cytokine that has been implicated in a number of pathophysiological states.[1] Thus inhibitors of ICE, the key enzyme that converts the inactive pro-IL-1β to the biologically active form, would be of pharmacological value.[2] Structurally, ICE inhibitors can be dissected into three components; a core fragment, a P4–P2 peptidomimetic head-fragment, and a prime side tail-fragment. We have recently reported[3] our efforts at delineating optimal binding fragments for the prime side. ICE has a key requirement for Asp as the core fragment[4] as revealed by SAR data buttressed by X-ray crystallography.[5] However, most SAR campaigns have truncated the prime side at the Asp carbonyl employing an acylal as a 'prodrug' (Fig. 1) focusing synthetic efforts at optimizing the P2–P4 segment.

Tetrapeptide Ac-YVAD-CHO (1, Fig. 2)[5a,6] is a potent competitive ICE inhibitor. The P1–P4 residues of **1** represent the natural binding amino acids exhibiting the obligatory P1 aspartic acid. This requirement for Asp at P1 is a consequence of its interaction with the oxy-anion hole formed by Arg341, Arg179, and Gln283. The remaining residues interact with the S2, S3, and S4 pockets utilizing the alanine methyl, valine isopropyl, and tyrosine phenol moieties, respectively.

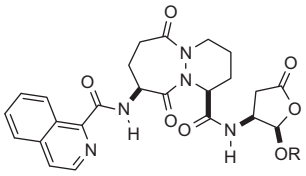

2a R=H (VRT-18858)
2b R=Et (VX-740)

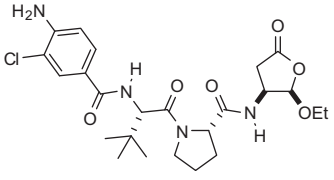

3 (VX-765)

This peptide inhibitor has been the epicenter of numerous optimization studies for more drug-like compounds. VX-740 (pralnacasan) **2b**,[7] prodrug of **2a**, and VX-765 **3**[8] are two examples of ICE inhibitors containing P2–P3 replacements that have embodied sufficient biopharmaceutical properties to merit clinical investigation. Both compounds leverage the requirement for aspartic acid (ethyl acylal prodrug form) at P1 and the pyridazinodiazepine and proline cores, respectively, of **2** and **3**, to effectively mimic the β-sheet H-bonding

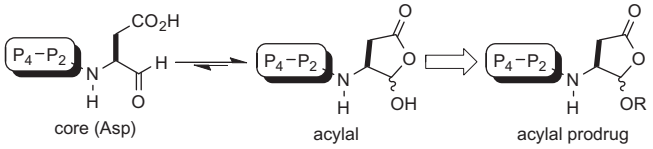

Figure 1. General structural features of an ICE inhibitor.

* Corresponding author at present address: Pfizer Global R&D, MS 8220-4225, Eastern Point Road, Groton, CT 06340, USA. Tel.: +1 860 686 9379.
E-mail address: paul.galatsis@pfizer.com (P. Galatsis).

0960-894X/$ - see front matter © 2010 Elsevier Ltd. All rights reserved.
doi:10.1016/j.bmcl.2010.07.004

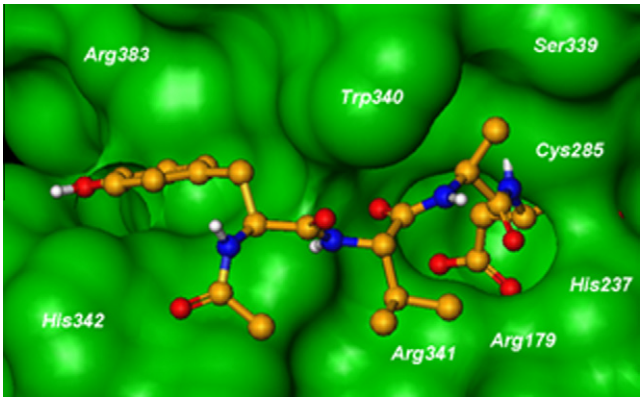

Figure 2. Binding pose of Ac-YVAD-CHO **1** with ICE.

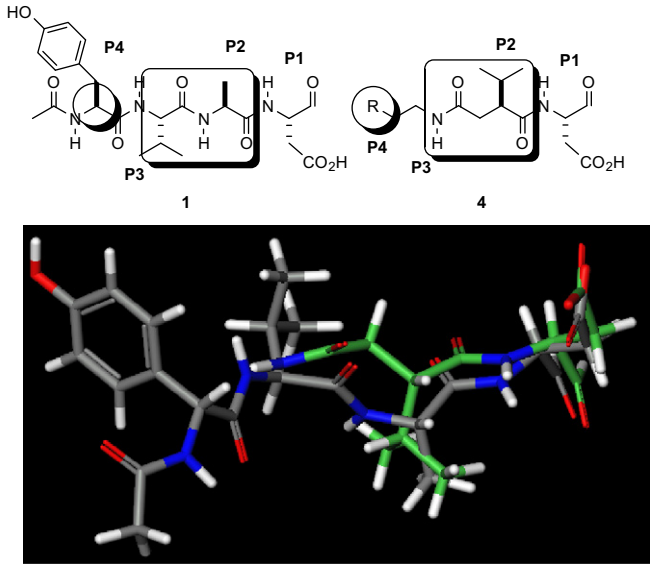

Figure 3. Top panel shows a comparison of P2–P4 residues. Bottom panel shows an overlay of **1** (gray) with **4** (green) truncated at P4.

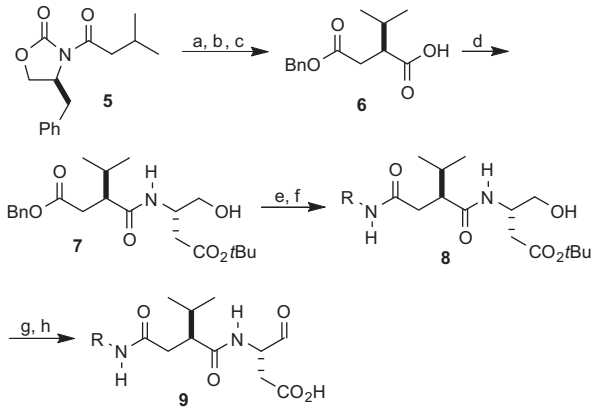

Scheme 1. Reagents: (a) NaHMDS; (b) $BrCH_2CO_2Bn$; (c) LiOH, H_2O_2; (d) $H_2NCH(CO_2tBu)CH_2OH$, EDCI, HOBt, NMM; (e) H_2, 20% Pd/C; (f) $ArCH_2CH_2NH_2$, EDCI, HOBt, NMM; (g) IBX; (h) TFA.

interactions observed from X-ray crystal structure data of **1** (Fig. 2),[5a] while removing several of the metabolically labile amide bonds.

We now report the identification of succinic acid amides **4** as suitable replacements for the P2–P3 fragment. Figure 3 provides a simplistic view toward the origins for these compounds. Upon visual comparison of the P2–P3 residues of **1** with the succinic acid moiety of **4**, our proposed scaffold replacement, the analogy becomes apparent. The P2 methyl group in **1** is now the isopropyl moiety of **4**.[9] Moreover, the P3 residue of **1** is directly related to the distal amide nitrogen, relative to the P1 aspartic acid, providing a synthetically amenable method for probing this chemical space. Finally, the R-group of **4** aligns with the P4 residue found in **1**. Thus, in a compact and more easily accessible synthetic framework, one can design and optimize ICE inhibitors with greater potential for clinically viability.

The desired target compounds **9**[10] could be obtained using a synthetic route starting with the known oxazolidinone **5** (Scheme 1).[11] Treating the enolate of **5**[11] with benzyl bromoacetate followed by removal of the chiral auxiliary afforded **6**. Diimide coupling of β-*t*-butyl ester alcohol of aspartic acid produced the corresponding amide alcohol **7**. Hydrogenolysis of the benzyl ester moiety followed by amide coupling installed the P4 substituent present in **8**. The synthetic protocol was completed by IBX oxidation of the alcohol to the corresponding aldehyde and deprotection of the *t*-Bu ester to generate the required P4 substituted carboxy aldehydes **9**.

With compound **9** in hand, their affinity for ICE was evaluated. Table 1 presents the results of the incorporation of substituted phenpropyl fragments at the P4 position. Overlays, as exemplified in Figure 3, indicated this was the best arrangement to access the region of P4 occupied by the phenoxy fragment of tyrosine. Data for **1** and **2a** have been included to serve as a benchmark for the novel compounds now being disclosed. Compound **9a** clearly indicated that potent ICE inhibitors could be obtained with our succinic acid amide P2–P3 scaffold replacement linked to a minimally elaborated P4 moiety. With this reference point, one could now systematically probe the SAR space for this template. Compound **9b** showed that substitution on the phenyl ring could be tolerated. While the oxo modification to the linker, present in **9c**, was tolerated, a sevenfold increase in potency was observed with an oxa-modification found in **9d**. The overlays (Fig. 3) also indicated that one could reach out to the S3 pocket by substituting off the distal amide (relative to **1**) nitrogen. The natural residue for P3 is valine, thus **9e** introduces an isopropyl group to this position which resulted in a sixfold loss in potency. However, it had been determined that the most potent arrangement of amino acid residues for the P1–P4 segment was WEHD and not the natural YVAD.[4] Compound **9f** introduces a propionic acid moiety at this position to mimic the glutamate found in this substrate. About a twofold increase in potency relative to **9d** was observed. Thus, we concluded that substitution at this position had minimal effects on potency but at the cost of physical–chemical properties.

Compound **9g** attempted to restrict the bond rotation of the linker and was found to be tolerated. Relative to **9d**, compound **9h** was 18-fold more potent. This compound took advantage of the knowledge that phenyl substitution was tolerated but now introduced a nitrogen atom in the linker in exchange for the oxygen atom. Interestingly, rigidifying the linker, as exemplified by **9i**, resulted in a dramatic loss in potency. Presumably, the linear conformation produced in this example indicated this was not the bioactive conformation. This observation was reinforced with **9j**. The compound maintains the core fragment found in **9a** but puts a kink in the linker with the introduction of the fused phenyl ring. It was observed from the crystal structure of **1** (Fig. 1) that the tyrosine at P4 must bend back toward the protein and **9j** reproduces this conformational requirement, such that, it exhibited a 200-fold improvement in potency, relative to **9a**.

Table 1
ICE enzyme inhibition data[a]

Entry	Structure	K_i (nM)	IC_{50} (nM)
1	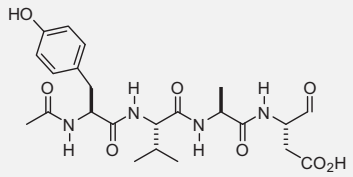	0.70	17
2a	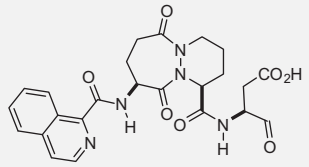	0.60	3.4
9a	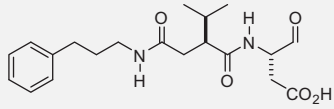	115	444
9b	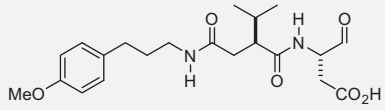	70.9	410
9c	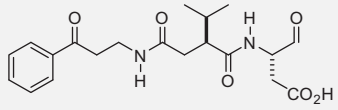	118	398
9d	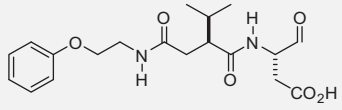	16.9	539
9e	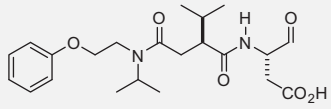	100	584
9f	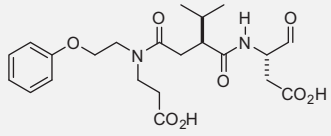	9.24	114
9g	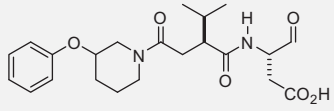	21.5	170
9h	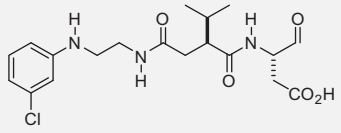	0.95	11.2
9i	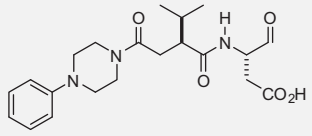	1020	7810
9j	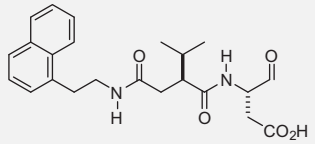	0.58	5.7

[a] For a description of the assay see Ref. 12. Values are the geometric mean of two or more experiments.

This last observation was the genesis of implementing the use of fused-bicyclic heteroaromatic ring systems for the P4 substituent. To this end, three related frameworks were examined, indoles, benzimidazoles, and quinolines. The modulation of affinity, one could explore with these scaffolds, could be conducted in a bifurcated manner. First, the presumed bioactive conformation would be maintained in a gross manner, but these systems introduce subtle variations that could be exploited. Secondly, the introduction of heteroatoms provides the ability to control physical–chemical properties that may lead to improved ADME profiles.

Table 2
ICE enzyme inhibition data[a]

Entry	Structure	K_i (nM)	IC_{50} (nM)
9k	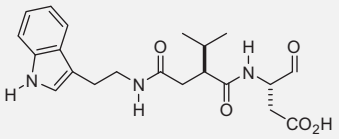	5.02	23.1
9l	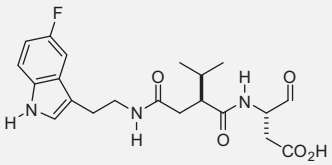	7.9	37
9m	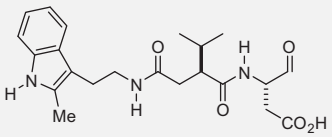	1.29	18
9n	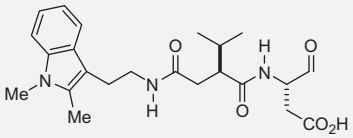	0.90	42.5
9o	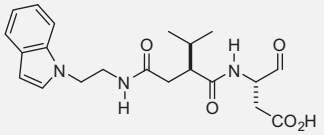	4.03	45.3

[a] For a description of the assay see Ref. 12. Values are the geometric mean of two or more experiments.

Table 2 presents the results obtained from incorporation of substituted indole fragments. Compound **9k** represents the indole equivalent to the naphthalene found in **9j** and was found to be about ninefold less potent. As was observed previously, substitution of the phenyl moiety was tolerated as exemplified by the 5-fluoro in **9l**. The 2-methyl substituent of **9m** afforded a fourfold increase in potency. An additional 1.4-fold potency increase was found with **9n** by the addition of a second methyl group to the 1-position of the indole ring. Switching the point of attachment of the fused bicyclic heterocycle, as presented in **9o**, was tolerated and did not have a dramatic effect.

The benzimidazole SAR is summarized in Table 3. Compound **9p** is the benzimidazole equivalent to **9j** or **9k** and was found to be about fourfold less potent than **9k**. As was observed in the previous series, substitution of the phenyl or imidazole ring was tolerated. Indeed, compounds **9q**–**9u** indicated that substitution of the phenyl or imidazole ring could recover this activity and **9t** indicated that fairly large groups could be accommodated at the imidazole 2-position without a dramatic loss in potency. While, in general, the SAR for these substitutions was fairly flat as most groups resulted in equipotent compounds, substitution on both rings, as shown in **9u**, provided the optimal substitution pattern and resulted in a compound of comparable potency to **9j** and **9m**.

The subtle nuances seen in this SAR provided the desire for a greater understanding of the binding interactions for this series of compounds. This greater insight was partially achieved when

Table 3
ICE enzyme inhibition data[a]

Entry	Structure	K_i (nM)	IC_{50} (nM)
9p	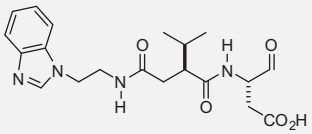	20	33.7
9q	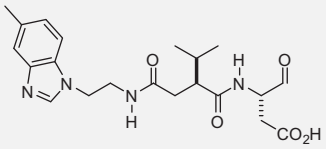	4.85	15.3
9r	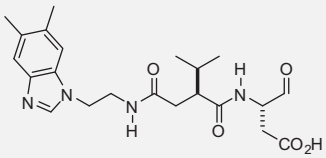	2.81	14.5
9s	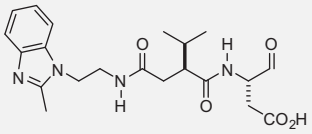	4.68	23.8
9t	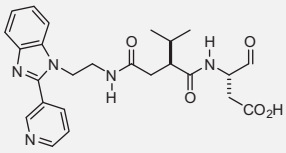	3.85	26.5
9u	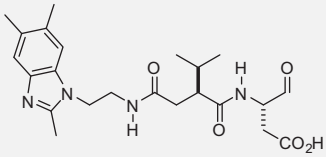	1.26	9.18

[a] For a description of the assay see Ref. 12. Values are the geometric mean of two or more experiments.

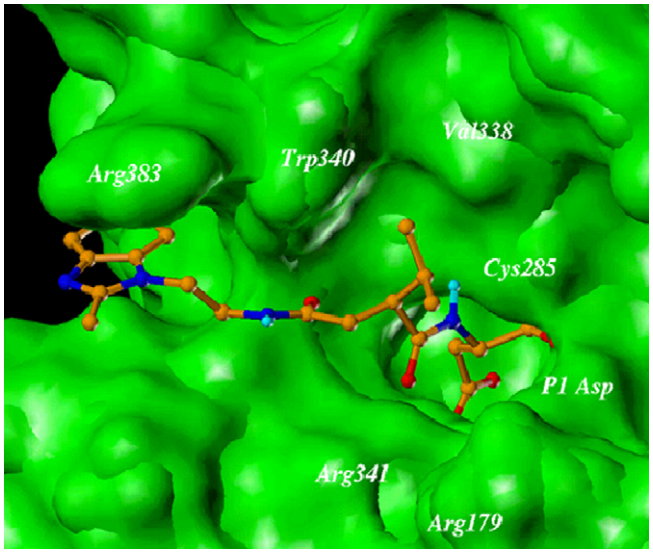

Figure 4. Docking pose for X-ray crystal structure of **9s** (3NS7).

an X-ray crystal structure of **9s** (3NS7) bound in the active site of ICE was determined (Fig. 4). As can be discerned from the binding pose, the Asp residue was found to be binding in the oxy-anion hole, as previously observed. The isopropyl substituent of the succinic acid amide P2–P3 scaffold replacement was found interacting with the S2 pocket, defined by Trp340 and Val338. While it appears the second methyl group of the isopropyl side chain was not making any apparent contacts, the ethyl variation of the succinic acid amide was found to be a less effective ICE inhibitor (data not shown).[9] As predicted, the succinic acid amide scaffold does not provide for any S3 interactions, and from this pose one would expect the amide nitrogen substituents to be pointing out into solvent. This is most likely the case for the *N*-*i*Pr substituent of **9e**, however, for **9f**, which incorporated an *N*-propionic acid substituent, the extended nature of this fragment presumably allowed it to make minimal contacts in S3. Finally, the benzimidazole moiety at P4 appears to be interacting with the Arg383 and confirms the kinked bioactive conformation, in that the interaction with S4 appears to be with the phenyl fragment.

The last P4 scaffold investigated was based on a quinoline group and is presented in Table 4. In this series, the SAR appears to be more tolerant of substitution and of comparable potency to the most potent indoles, **9n**, and benzimidazoles, **9u**. Compounds **9v**,

Table 4
ICE enzyme inhibition data[a]

Entry	Structure	K_i (nM)	IC_{50} (nM)
9v	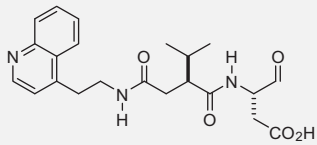	1.31	4.77
9w	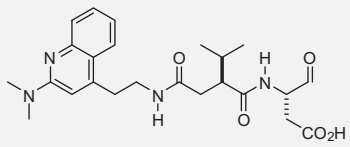	3	3.61
9x	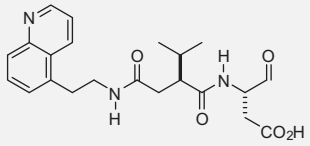	1.81	5.81
9y	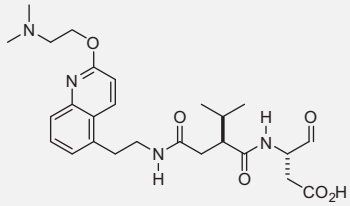	16.7	102
9z	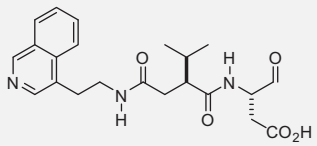	4.3	12

[a] For a description of the assay see Ref. 12. Values are the geometric mean of two or more experiments.

Table 5
Comparison of in vitro and in vivo data

Entry	muK_i (nM)	muK_i/huK_i	PBMC (IC_{50} μM)	huSCID (%)
1	9.0	12.8	1.2	69
2a	7.0	11.7	0.38	62
9m	13.4	10.3	1.50	54
9s	18.7	3.98	2.90	68
9x	14.4	8.0	0.65	52

a 4-quinolinyl-analog, and **9x**, a 5-quinolinyl-analog, are equipotent. An obvious exception was **9y** which exhibited a 12.7-fold loss in potency by the incorporation of a dimethylamino-ethoxy substituent at the 2-position of the quinoline ring.

Having identified potent compounds in each P4 variant, one compound from each series was selected for additional profiling. Table 5 presents the differences inherent in these compounds. The first point of differentiation was related to species specificity and the ability to use in vivo models. Since the compounds were optimized for human potency, the differences between the human and mouse isoforms of ICE could be determined and were found to be significant (4- to 10-fold weaker) which resulted in the necessity of using the in vivo huSCID model.[13] The second point of differentiation was related to a dramatic loss of potency observed for these compounds in going from the enzyme assay to cell-based assay formats (e.g., PBMC[14]), which was not unique to our compounds. Presumably, ionization of the carboxylic acid reduces the permeability giving rise to the observed potencies. Despite this disconnect, significant IL-1β reduction was observed in the in vivo huSCID model.[13] In addition to the species selectivity that was observed, we also determined that these compounds showed selectivity across several members of the caspase enzyme family. Along with caspase 1, caspase 3, 4, 6, and 8 activity was determined. While **2a** showed a minimum of 53-fold selectivity over these enzymes, our compounds exhibited greater than 200-fold selectivity for these caspases, thereby providing a wider therapeutic index against these targets.

In following up with PK studies, it was observed that these compounds did not all behave in a similar manner. Figure 5 clearly shows that **9x** has comparable exposure to **2a** and better exposure than **9s**, which essentially had no oral bioavailability. In the cases of **2b** and **3**, there were clear benefits, from a bioavailability perspective, for advancing the acylal prodrug version of the inhibitor. Based on this and other data, a systematic exploration of prodrugs for these compounds was pursued.

We began our prodrug approach by initiating studies focused on gaining an understanding into the various forms of the acylal prodrugs. A simple ^{1}H NMR experiment was conducted to chemically assess the potential species that this moiety could participate (Fig. 6). Taking Asp-CHO **10** in water or methanol, the chemical shift

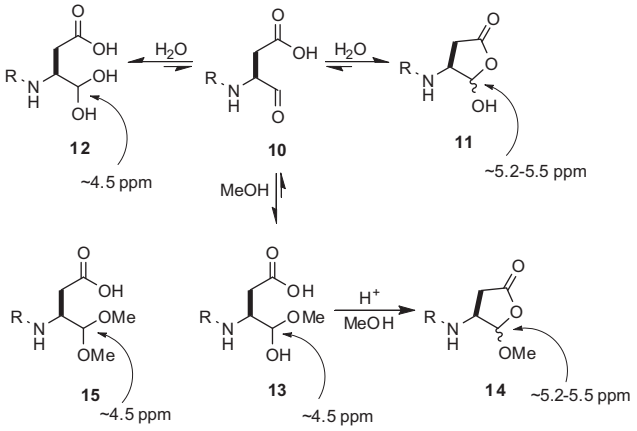

Figure 6. Summary of ^{1}H NMR experiments looking to decipher the various prodrug acylal species that could exist in solution.

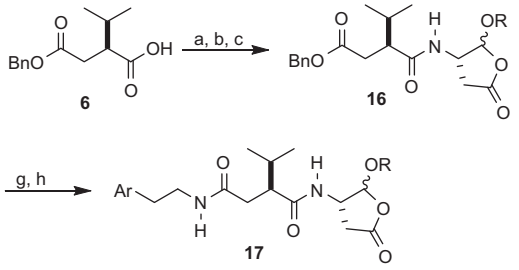

Scheme 2. Reagents: (a) $H_2NCH(CO_2tBu)CH_2OH$, EDCI, HOBt, NMM; (b) IBX; (c) TFA, ROH with chromatography to separate diastereomers; (d) H_2, 20% Pd/C; (f) $ArCH_2CH_2NH_2$, EDCI, HOBt, NMM.

for the acetal methane hydrogen was determined and correlated with structural substitution features. From this analysis, the predominant isomer in methanol-d_4 was the acyclic hemi-acetal **13** and not **11** nor was it methyl acylal **14**. What was observed was a mix of diastereomers with two acetal methine doublets at ~4.5 ppm. Based on the chemical shifts of cyclic acylal intermediates

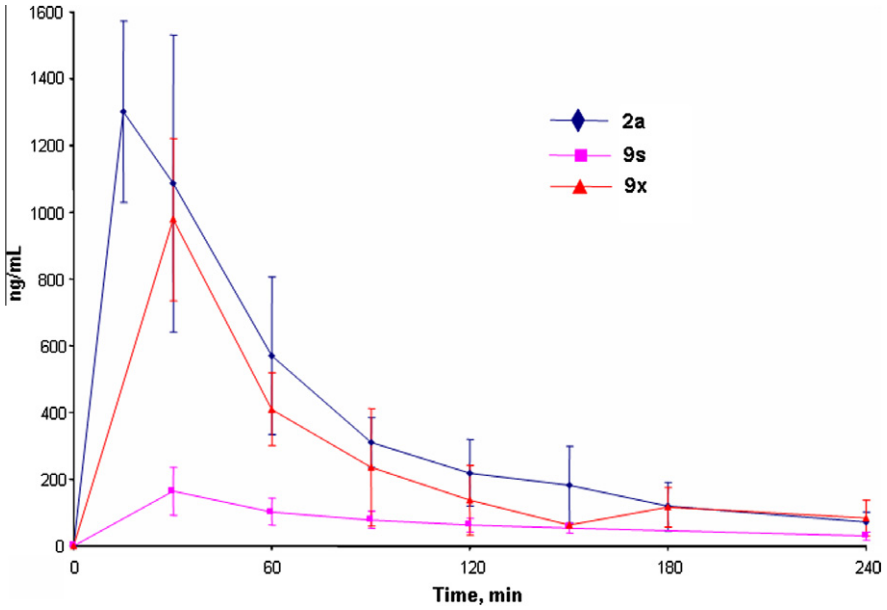

Figure 5. Bioavailability for selected compounds. Wistar rats were dosed 25 mg/kg po using a vehicle of 10% DMSO, 11.25% Trappsol, D5W and the compounds were detected by LC/MS.

Table 6
Comparison of in vivo half-lives of selected compounds

Entry	Structure	$t_{½}$ (h)
2b	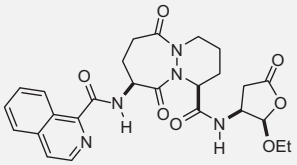	0.87
17a	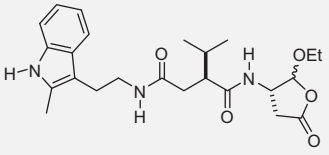	1.27
17b	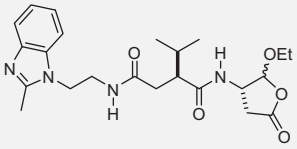	1.60
17c	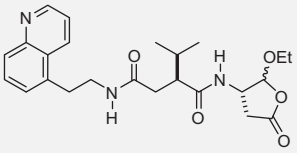	0.87

Table 7
Effect of compound stereochemistry on plasma stability

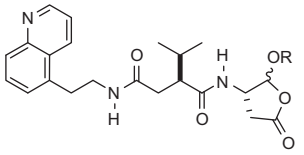

Entry	R group	Stereochem	$t_{½}$ (h)
17d	Et	*cis*	0.87
17e		*trans*	4.3
17f	*n*Pr	*cis*	2.0
17g		*trans*	10.0
17h	(*S*)-*s*Bu	*cis*	3.9
17i		*trans*	7.7
17j	Cyclopentyl	*cis*	5.1
17k		*trans*	15.7

like **14** (~5.2–5.5 ppm) and of the acyclic acetal **15** (~4.5 ppm), it appears clear that the species seen for the parent prodrug in methanol-d_4 was the hemi-acetal **13**.

We were able to access a variety of the acylal prodrugs by modifying the original synthetic protocol to that presented in Scheme 2. One could readily separate the diastereomers, by chromatography, thus not only could the effect of substituents be investigated for these prodrugs but also stereochemical implications could be probed.

Following the examples of **2b** and **3**, we synthesized the ethyl acylal prodrugs of our representative examples with Table 6 presenting the human plasma stability of these compounds. The immediate observation one can make is that plasma stability of the prodrug is not dependent upon the nature of the P4 substituent or the P2–P3 scaffold, since both **2b** and **17a**, **17b**, and **17c** were

Table 8
Comparison of compound bioavailability data

Entry	Structure	%*F*
2b	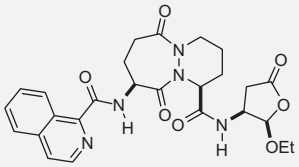	
17d	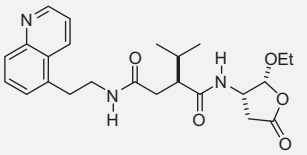	25
17f	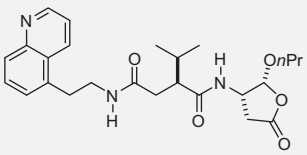	9
17g	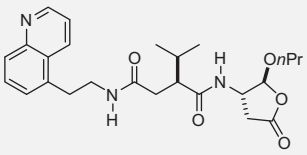	35
17j	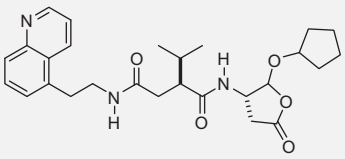	5

determined to have similar stabilities in vivo. More likely, this is a reflection of the stability of acylal moiety under the conditions found in vivo and indicates one may be able to modulate pharmacokinetic properties by suitable modification of the acylal group.

With this data in hand, we next focused our attention to understanding the effect of the prodrug substituent on plasma stability. Table 7 presents the results of these studies. For each acylal prodrug, two possible stereoisomers are possible; *cis* and *trans* relative to the lactone ring fragment. The first general trend observed was that the *trans* isomer appeared to be more stable in plasma compared to the *cis* stereoisomer. The second trend observed was related to the steric bulk of the prodrug substituent. As this group increased in size, irrespective of the stereochemistry, the stability of the prodrug increased. Thus one could use this SAR to modulate the biopharmaceutical properties of the drug to fit the desired indication, that is, short or long plasma half-life.

Combining all this data, we prepared several compounds within this series and determined the bioavailability as part of a decision-making process for moving a compound forward into clinical development (Table 8). While most of the compounds examined had very poor oral bioavailability, we found that **17f** was comparable to **2b**, a compound Vertex had moved into clinical development.

In summary, we have identified a P2–P3 replacement fragment that retains high in vitro potency but in a readily synthesizable succinic acid moiety. This scaffold was also found to inhibit the production of IL-1β in an in vivo model. While it was determined that the parent compound did not have biopharmaceutical properties sufficient for progression into development, a prodrug approach was pursued as a solution to this issue. It was determined that **17f** had properties comparable to **2b** and was identified as a potential candidate for clinical development.

References and notes

1. (a) Thornberry, N. A.; Bull, H. G.; Calaycay, J. R.; Chapman, K. T.; Howard, A. D.; Kostura, M. J.; Miller, D. K.; Molineaux, S. M.; Weidner, J. R.; Aunin, J.; Elliston, K. O.; Ayala, J. M.; Casano, F. J.; Chin, J.; Ding, G. J.-F.; Egger, L. A.; Gaffney, E. P.; Limjuco, G.; Palyha, O. C.; Raju, S. M.; Rolando, A. M.; Salley, J. P.; Yamin, T.-T.; Lee, T. D.; Shively, J. E.; MacCross, M.; Mumford, R. A.; Schmidt, J. A.; Tocci, M. J. *Nature* **1992**, *356*, 768; (b) Thornberry, N. A. *Br. Med. Bull.* **1996**, *53*, 478; (c) Talanian, R. V.; Brady, K. D.; Cryns, V. L. *J. Med. Chem* **2000**, *43*, 3351; (d) Bird, S.; Zou, J.; Wang, T.; Munday, B.; Cunningham, C.; Secombers, C. J. *Cytokine Growth Factor Rev.* **2002**, *13*, 483; (e) Joosten, L. A. B.; van den Berg, W. B. *Drug Discovery Today* **2006**, *3*, 169.
2. (a) Ator, M. A.; Dolle, R. E. *Curr. Pharm. Des.* **1995**, *1*, 191; (b) Giegel, D. A.; Kostlan, C. R. *Annu. Rep. Med. Chem.* **1998**, *33*, 183; (c) Talanian, R. V.; Brady, K. D.; Cryns, V. L. *J. Med. Chem.* **2000**, *43*, 3351; (d) Ashwell, S. *Expert Opin. Ther. Pat.* **2001**, *11*, 1593; (e) Randle, J. C. R.; Harding, M. W. H.; Ku, G.; Schonharting, M.; Kurrle, R. *Expert Opin. Invest. Drugs* **2001**, *10*, 1207; (f) Braddock, M.; Quinn, A. *Nat. Rev. Drug Disc.* **2004**, *3*, 1; (g) Dinarello, C. A. *Curr. Opin. Pharmacol.* **2004**, *4*, 378; (h) Le, G. T. E.; Abbenante, G. *Curr. Med. Chem.* **2005**, *12*, 2963; (i) Fischer, U.; Schulze-Osthoff, K. *Pharmacol. Rev.* **2005**, *57*, 187.
3. Galatsis, P.; Caprathe, B.; Downing, D.; Gilmore, J.; Harter, W.; Hays, S.; Kostlan, C.; Linn, K.; Lunney, E.; Para, K.; Thomas, A.; Warmus, J.; Allen, H.; Brady, K. D.; Walker, N. *Bioorg. Med. Chem. Lett.* **2010**, *20*, 5089.
4. (a) Thornberry, N. A.; Molineaux, S. M. *Protein Sci.* **1994**, *4*, 3; (b) Rano, T. A.; Timkey, T.; Peterson, E. P.; Rotonda, J.; Nicholson, D. W.; Becker, J. W.; Champman, K. T.; Thornberry, N. A. *Chem. Biol.* **1997**, *4*, 149; (c) Chereau, D.; Kodandapani, L.; Tomaselli, K. J.; Spada, A. P.; Wu, J. C. *Biochemistry* **2003**, *42*, 4151.
5. (a) Wilson, K. P.; Black, J. F.; Thomson, J. A.; Kim, E. E.; Griffith, J. P.; Navia, M. A.; Murcko, M. A.; Chambers, S. P.; Aldape, J. P.; Raybuck, S. A.; Livingston, D. J. *Nature* **1994**, *370*, 270; (b) Walker, N. P. C.; Talanian, R. V.; Brady, K. D.; Dang, L. C.; Bump, N. J.; Ferenz, C. R.; Franklin, S.; Ghayur, T.; Hackett, M. C.; Hammill, L. D.; Herzog, L.; Hugunin, M.; Houy, W.; Mankovick, J. A.; McGuiness, L.; Orlewicz, E.; Paskind, M.; Pratt, C. A.; Reis, P.; Summani, A.; Terranova, M.; Welch, J. P.; Moller, A.; Tracey, D. E.; Kamen, R.; Wong, W. W. *Cell* **1994**, *78*, 343.
6. (a) Chapman, K. T. *Bioorg. Med. Chem. Lett.* **1992**, *2*, 613; (b) Boost, K. A.; Hoegel, S.; Hofstetter, C.; Flondor, M.; Stegewerth, K.; Platacis, I.; Pfeilschifter, J.; Muhl, H.; Zwissler, B. *Intensive Care Med.* **2007**, *33*, 863.
7. (a) Rudolphi, K.; Gerwin, N.; Verzijl, N.; van der Kraan, P.; van den Berg, W. *Osteoarthritis Cartilage* **2003**, *11*, 738; (b) Bauer, C.; Loher, F.; Dauer, M.; Mayer, C.; Lehr, H. A.; Schonharting, M.; Hallwachs, R.; Endres, S.; Eigler, A. *Dig. Dis. Sci.* **2007**, *52*, 1642.
8. Wannamaker, W.; Davies, R.; Namchuk, M.; Pollard, J.; Ford, P.; Ku, G.; Decker, C.; Charifson, P.; Weber, P.; Germann, U. A.; Kuida, K.; Randle, J. C. R. *J. Pharmacol. Exp. Ther.* **2007**, *321*, 509.
9. Other substituents were investigated (data not shown) and the isopropyl was determined to be optimal. For example, cyclopentyl and cyclohexyl afforded a fivefold loss in potency. A free hydroxyl at this position lost activity, while ethers and esters regained some of the activity (~500 nM) and amides and carbamates also showed a dramatic loss of potency.
10. All compounds were characterized by ^{1}H NMR, MS, and were >98% pure by either CHN analysis or analytical HPLC.
11. Evans, D. A.; Britton, T. C.; Dorow, R. L.; Delaria, J. F., Jr. *Tetrahedron* **1988**, *44*, 5525. This compound is also commercially available.
12. Brady, K. D. *Biochemistry* **1998**, *37*, 8508.
13. Since compounds were optimized for human ICE and were found to be less potent in mice, the huSCID assay was developed to understand in vivo activity. Severe combined immuno-deficient (SCID) mice were injected with human PMBC cells 15 min before the start of the experiment. At time zero, the mice were treated with 5 mg/kg of LPS iv followed by the compound of interest dosed at 3 mg/kg iv 15 min before bleeding at the 2 h time point. The blood taken was analyzed for various parameters. These included measuring the levels of human cytokines, mouse cytokines and for the compound itself.
14. Human peripheral blood mononuclear cells (PBMC) were isolated from heparinized blood by centrifugation over a Ficoll cushion and then washed three times with PBS. The PBMC's were suspended in a medium containing RPMI 1640 with glutamine, penicillin, streptomycin, and 2% human AB serum and then plated at 106 cells per well in a 96-well flat bottom plate. PBMC's were stimulated overnight with 10 ng/mL of LPS in the presence or absence of inhibitor. The medium was harvested and the level of mature IL-1β was determined using an ELISA kit from R&D Systems. Compound inhibition (IC_{50} values) was assessed by determining the concentration of agent which reduced IL-1β levels by 50%.